



Optimization of mechanical properties, biocorrosion properties and antibacterial properties of wrought Ti-3Cu alloy by heat treatment

Mianmian Bao^a, Ying Liu^a, Xiaoyan Wang^b, Lei Yang^a, Shengyi Li^a, Jing Ren^a, Gaowu Qin^a, Erlin Zhang^{a,*}

^a School of Materials Science and Engineering, Key Lab. for Anisotropy and Texture of Materials, Education Ministry of China, Northeastern University, Shenyang, 110819, China

^b School of Metallurgy, Northeastern University, Shenyang, 110819, China

ARTICLE INFO

Article history:

Received 2 December 2017

Received in revised form

25 January 2018

Accepted 26 January 2018

Available online 3 February 2018

Keywords:

Ti-Cu alloy

Heat treatment

Microstructure

Mechanical properties

Corrosion resistance

Antibacterial properties

ABSTRACT

Previous study has shown that Ti-3Cu alloy shows good antibacterial properties (>90% antibacterial rate), but the mechanical properties still need to be improved. In this paper, a series of heat-treatment processes were selected to adjust the microstructure in order to optimize the properties of Ti-3Cu alloy. Microstructure, mechanical properties, biocorrosion properties and antibacterial properties of wrought Ti-3Cu alloy at different conditions was systematically investigated by X-ray diffraction, optical microscope, scanning electron microscope, transmission electron microscopy, electrochemical measurements, tensile test, fatigue test and antibacterial test. Heat treatment could significantly improve the mechanical properties, corrosion resistance and antibacterial rate due to the redistribution of copper elements and precipitation of Ti₂Cu phase. Solid solution treatment increased the yield strength from 400 to 740 MPa and improved the antibacterial rate from 33% to 65.2% while aging treatment enhanced the yield strength to 800–850 MPa and antibacterial rate (>91.32%). It was demonstrated that homogeneous distribution and fine Ti₂Cu phase plays a very important role in mechanical properties, corrosion resistance and antibacterial properties.

© 2018 The Authors. Production and hosting by Elsevier B.V. on behalf of KeAi Communications Co., Ltd. This is an open access article under the CC BY-NC-ND license (<http://creativecommons.org/licenses/by-nc-nd/4.0/>).

1. Introduction

Titanium and titanium alloys have been widely used in the biomedical implant field due to their excellent mechanical properties and biocompatibility [1,2], especially in repair and replacement materials such as artificial joint and dental implants [3,4]. But one of the big problems that plague the doctor is the infection or the inflammation. Once the infection occurs, it will seriously affect the healing process. Patients sometimes need to accept long-term antibiotic treatment even re-operation. Thus, the implant with strong antibacterial properties shows great potential for medical implant materials in clinic application.

Recently, many researches have been reported on the surface modification of titanium alloy to obtain good antibacterial properties. But surface coatings are susceptible to exfoliation and the

antibacterial effect is greatly reduced over the time [5–8]. Alternatively, alloy-type antimicrobial titanium alloys in which antimicrobial elements are distributed uniformly have attracted much attention worldwide due to their long-term antibacterial property, good wear resistance, good corrosion resistance. Shirai et al. [9] first reported that titanium alloys containing 1% Cu and 5% Cu have antimicrobial activity and substantially reduce the incidence of pin tract infection. Then, Ti–Cu sintered alloy with 5 wt% or high Cu exhibits a strong and stable antibacterial rate (>99%) against *S. aureus* and *E. coli* [10,11]. Recently, ingot metallurgy as well as subsequent metal forming processing has been used to produce antibacterial titanium, such as Ti-6Al-4V-xCu (X = 1, 3, 5 wt%) [12], Ti-5Cu and Ti-10Cu [13], and Ti-Cu alloys with 2–4 wt% Cu [14]. Both Ti-Cu sintered alloy and Ti-Cu ingot alloy show excellent cytocompatibility and have no influence on the cell proliferation and differentiation [15,16]. It has been reported that the content of Cu and the existing form of Cu element had great influence on the antibacterial properties of Ti-Cu alloy. In order to get good antibacterial rate (>90%), the Cu content in Ti-Cu alloy has to be at least

* Corresponding author.

E-mail address: zhangel@atm.neu.edu.cn (E. Zhang).

Peer review under responsibility of KeAi Communications Co., Ltd.

3 wt% [10,14].

However, for biomedical application, metallic materials should also have good mechanical properties as well as good corrosion resistance. Yao et al. [17] prepared Ti–2.5Cu alloy through hot rolling and indicated that acicular Ti_2Cu particles with tens of nanometers in width and 100 nm in length contribute greatly to the strength. Souza [18] found that cooling rate higher than $9^\circ C/s$ leads to the formation of the α -Ti and smaller Ti_2Cu spheres (~5 nm diameter), and the hardness was improved greatly due to the existence of nanoscale Ti_2Cu phases. Our previous study also reported that homogeneously dispersed and fine Ti_2Cu would provide strong strengthening effect, good corrosion resistance and strong antibacterial ability [13,14,19]. All these indicate the shape and size of Ti_2Cu phase significantly influences the antibacterial properties and mechanical properties as well corrosion properties.

It has shown that Ti-3wt%Cu alloy exhibited comprehensive high antibacterial, high ductility and strength [14], therefore, Ti-3 wt.% Cu was prepared in this paper by ingot metallurgy followed by forging. It was proposed to obtain good corrosion resistance and mechanical properties of Ti-3Cu alloy by adjusting the existing form of Ti_2Cu phase without reduction in antibacterial properties. The primary results demonstrate that the mechanical properties, bio-corrosion resistance and the antibacterial ability of Ti-3Cu alloy could be improved by microstructure control through proper heat treatment. In comparison with pure titanium and Ti-6Al-4V, it was suggested that Ti-3Cu with good comprehensive properties could be a candidate for long-term implant.

2. Experimental

2.1. Preparation of samples

Ti-3Cu bar with 15 mm in diameter was used. Different heat treatments were used to change the microstructure, as listed in Table 1. Samples for the following test were sliced from the bar.

2.2. Phase identification and microstructure observation

Phase identification was conducted on an X-ray diffraction (XRD) at an accelerating voltage of 40 kV and a current of 40 mA. For microstructure observation, all samples were ground by SiC sandpapers up to 2000 grits, polished with 1 μm polishing paste and etched with Keller's solution consisting of 1 vol% HF acid, 2.5 vol% HNO_3 acid, 1.5 vol% HCl acid and 95 vol% H_2O . Microstructure was observed on an optical microscopy (OM, Olympus GX71) and scanning electron microscopy (SEM, JSM-6510A) with an energy-dispersive X-ray spectrometer (EDS). Samples for TEM observation were manually ground to 100 μm , punched into $\Phi 3mm$ discs and then ground to 50 μm with 1500 SiC sandpaper, and then ion milled at a low angle between 4° and 8° , finally observed under a transmission electron microscopy (TEM, JEOL-JEM2100).

2.3. Tensile test and fatigue test

Tensile specimen was 2 mm in thickness, 30 mm in length, with

a head width of 6 mm. The tensile testing was carried out on an electronic universal testing machine (AG-Xplus100 KN) with a crosshead speed of 0.5 mm/min. At least three samples were tested for each condition.

Fatigue performance of Ti-3Cu(T6-16) was tested on INSTRON 8801. Specimen were prepared in accordance with National Standards and Requirements GB3075-82 [20] and ASTM E 466-96 (Reapproved 2002) [21], the minimum cross-sectional area is 6 mm in diameter, the parallel section length is 18 mm, the radius of the transition arc is 30 mm and the clamping end is 12 mm in diameter. Before test, all samples were surface polished to ensure the surface roughness $Ra \leq 0.5 \mu m$. The samples were tested by up-and-down test method [22] at a stress ratio of $R = -1$, at the frequency of 20 Hz in $20^\circ C$.

2.4. Electrochemical test

Samples for electrochemical tests were put into a polymer sample holder with only one side of 12 mm in diameter exposed [23]. The test was conducted on a beaker containing 0.9% NaCl at $37 \pm 1^\circ C$ using Versa STAT V3 automatic laboratory corrosion measurement system (Princeton Applied Research, USA). According to ISO 10271:2001 Standard [24], the open-circuit potential vs. time curve (OCP curve) was recorded for up to 3600 s to determine the open circuit potential (E_{OCP} at 3600 s). After the OCP measurement, the EIS test was carried out at an open circuit potential with a 10 mV amplitude sine wave potential and a frequency range of 10^{-2} Hz to 10^5 Hz. Then Tafel curve was recorded at a scanning range of $-0.5 V \sim +1.5 V$ (relative to open circuit potential) and the scanning rate was $1 mVs^{-1}$. The Nyquist plot and Bode phase diagrams was analyzed and fitted by the ZsimpWin software. Three samples were measured at each condition. The corrosion rate (V) was calculated by Ref. [23]:

$$V = M i_{corr} / nF \quad (1)$$

where, M is the molar mass of titanium ($g mol^{-1}$), i_{corr} is the average corrosion current density measured in the electrochemical tests ($A cm^{-2}$), F is Faraday constant ($96,485 C mol^{-1}$) and n is the valence of titanium.

Table 1
Samples and heat treatment processing.

Samples	Conditions	Processing
Ti-3Cu(F)	F	As-forged and annealed
Ti-3Cu(T4)	T4	$900^\circ C/5 h$
Ti-3Cu(T6-16)	T6-16	$900^\circ C/5 h + 400^\circ C/16 h$
Ti-3Cu(T6-24)	T6-24	$900^\circ C/5 h + 400^\circ C/24 h$
Ti-3Cu(T6-36)	T6-36	$900^\circ C/5 h + 400^\circ C/24 h + 475^\circ C/12 h$

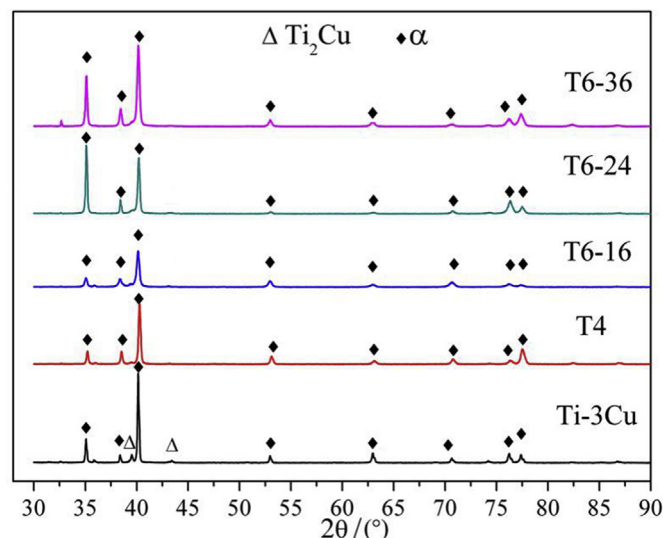


Fig. 1. XRD patterns of Ti-3Cu alloy under different heat-treatments.

2.5. Antibacterial properties

A plate-count method was used to assess the antibacterial properties of Ti–Cu samples. According to China Standard GB/T 2591 (equivalent to JIS Z 2801-2000, ASTM G21-96, and NEQ) [25], 12-multiwell culture plate, glass dishes and samples were sterilized at 121 °C for 30 min or with UV irradiation for 1 h. After that, the samples were placed in 12-multiwell culture plate with one sample in one well. 0.1 mL bacterial suspension (*S. aureus* concentration of 1.0×10^5 CFU/mL) was dripped onto the sample evenly so that the bacteria and the sample were in full contact. Then, the plate with samples and bacteria suspension was incubated at a relative humidity of 90% and 37 ± 1 °C for 24 h. After that, the sample was washed repeatedly and fully by 5 mL sterilized physiological saline solution to make sure that no bacterium was left on the samples. After thoroughly mixing, 100 μ L above washing solution was

pipetted on a nutrient agar plate and spread evenly, and then incubated at 37 °C for 24 h. The experiment was repeated at least 5 times. Then calculated antibacterial rate, R, defined by the following formula, was used to evaluate the antibacterial effect:

$$R = (N_{\text{control}} - N_{\text{sample}}) / N_{\text{control}} \times 100\% \quad (2)$$

where, N_{control} and N_{sample} are the average numbers of the bacterial colonies on the control sample (cp-Ti) and Ti–3Cu samples, respectively.

3. Results

3.1. Microstructure

Fig. 1 shows XRD patterns of Ti–3Cu alloys under different

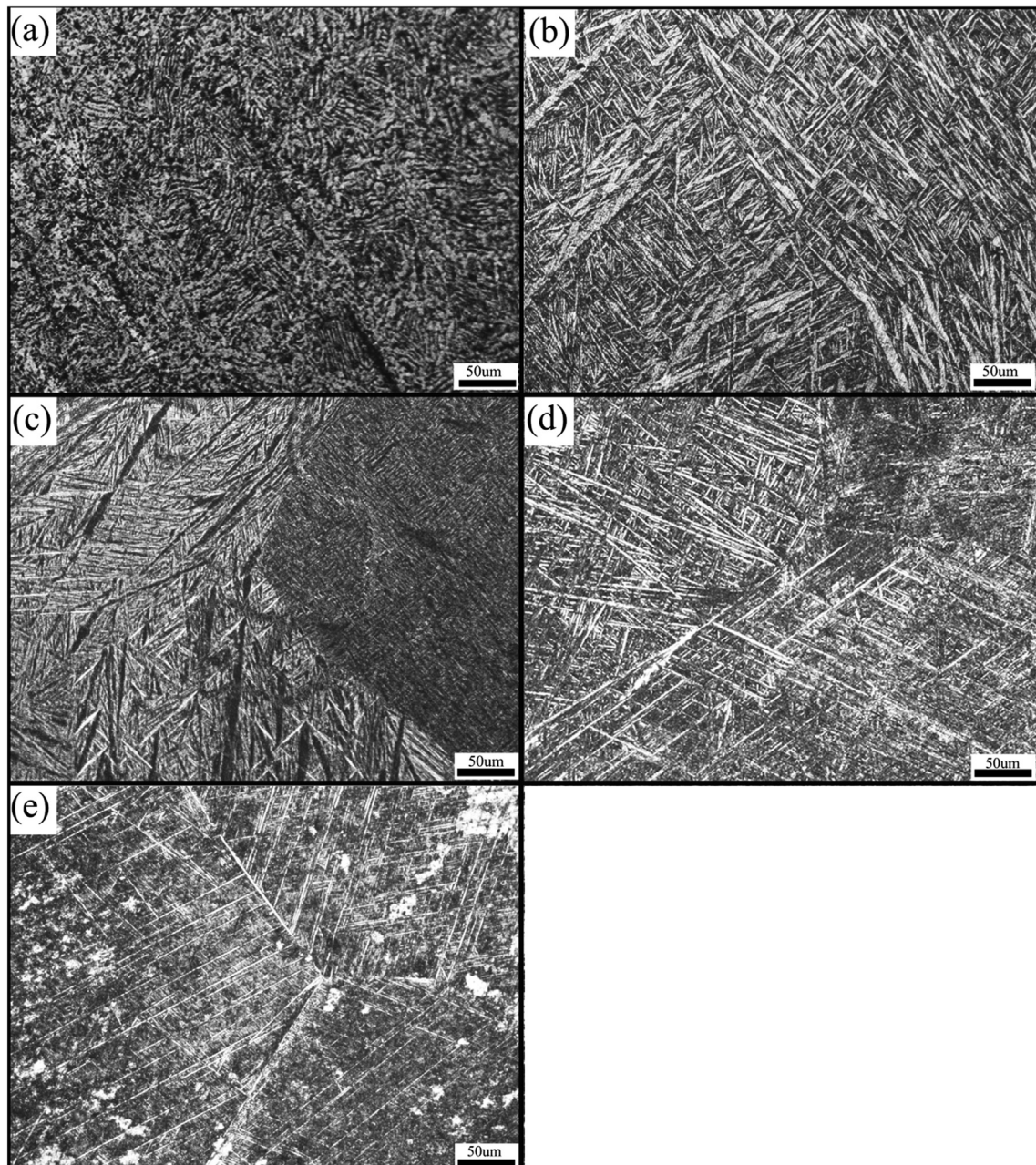


Fig. 2. Optical micrograph of Ti–3Cu alloys under different heat treatments. (a) F, (b) T4, (c) T6-16, (d) T6-24, (e) T6-36.

conditions. The diffraction peaks of α -Ti and Ti_2Cu were detected in Ti-3Cu(F), indicating that the forged Ti-3Cu alloy was mainly composed of two phases: α -Ti phase and Ti_2Cu phase. After the solid solution treatment (T4), the diffraction peak of Ti_2Cu phase disappeared, indicating that Ti_2Cu phase was completely dissolved in the matrix. After T6 treatments, no diffraction peak of Ti_2Cu phase was detected.

Fig. 2 shows the optical micrograph of Ti-3Cu alloys at different conditions. In Ti-3Cu(F) alloy, as shown in Fig. 2a, the grain boundary was difficult to be seen clearly due to the fine grain. The microstructure mainly consisted of fine lamellar α -Ti phase structure and broken basket-like microstructure distributed irregularly. After T4 treatment, Fig. 2b, typical acicular martensite with different sizes was observed on the matrix. After T6-16 treatment, Fig. 2c, no difference was found in optical microstructure in comparison with that of Ti-3Cu(T4) alloy, but the thick martensite structure was observed to be tapering with the aging time, which indicates the second phase gradually precipitated. After T6-24 treatment, as shown in Fig. 2d, the martensite structure was gradually reduced and α -Ti phases became shorter and narrower. Fig. 2e shows the microstructure of Ti-3Cu(T6-36) alloy. White cluster on the matrix surface was observed, which can be account for more α phase growing up and tending to be regular, growing in a certain direction and gradually being coarsen.

Fig. 3 shows SEM microstructure of Ti-3Cu(F) and Ti-3Cu(T4) alloys. As shown in Fig. 3a and b, the lamellar α -structure was clearly observed in Ti-3Cu(F), while Cu element located at the lamellar structure. The inserted high magnification SEM microstructure shows there are some particles with a diameter of about 200 nm distributed on the matrix. The EDS results (not shown here) indicated that point A mainly consisted of Cu and Ti elements with

an atom ratio of Ti to Cu of about 2, corresponding to Ti_2Cu phase in the XRD pattern in Fig. 1 After T4 treatment, as shown in Fig. 3c and d, the Cu element was more uniformly distributed on the matrix. The EDS results displayed the Cu content at Point C was about 1.9 wt% and the Cu content at Point B was about 2.78 wt%, slighter higher than the value at Point C, suggesting that Cu element nearly completely dissolved in titanium matrix after T4 treatment.

Fig. 4 shows TEM microstructure of Ti-3Cu alloys under different aging treatments. After T6-16 treatment, the lath-like α -Ti phases grew from the grain boundary and distributed regularly, as shown in Fig. 4a. In addition, there are some spherical phases with a diameter ≤ 10 nm around and in the lath-like α -Ti phases. Through the selected diffraction pattern, as shown in Fig. 4b, it can be concluded that the phases were Ti_2Cu phase precipitated from matrix during T6 treatment. With the extension of the aging duration to 24 h, the lath α -Ti phases became wider and longer obviously, as shown in Fig. 4c. In addition, Ti_2Cu phase grew up to about 20–40 nm and the shape changed to spherical or granular shape, as shown in Fig. 4d. After T6-36 treatment, in Fig. 4e, the lath-like α -phase became wider. High magnification TEM microstructure in Fig. 4f showed a typical granular-like eutectoid Ti_2Cu phase with a width of 30 nm and a length of about 100 nm, indicating that Ti_2Cu phase grew up significantly.

3.2. Tensile properties and fatigue properties

Fig. 5 shows the tensile properties of Ti-3Cu alloys after different heat treatments. A large plastic deformation zone was seen obviously in the tensile stress-strain curve of Ti-3Cu(F) alloy, which displays that Ti-3Cu(F) alloy has very good plasticity. After T4 treatment, the yield strength and tensile strength was increased

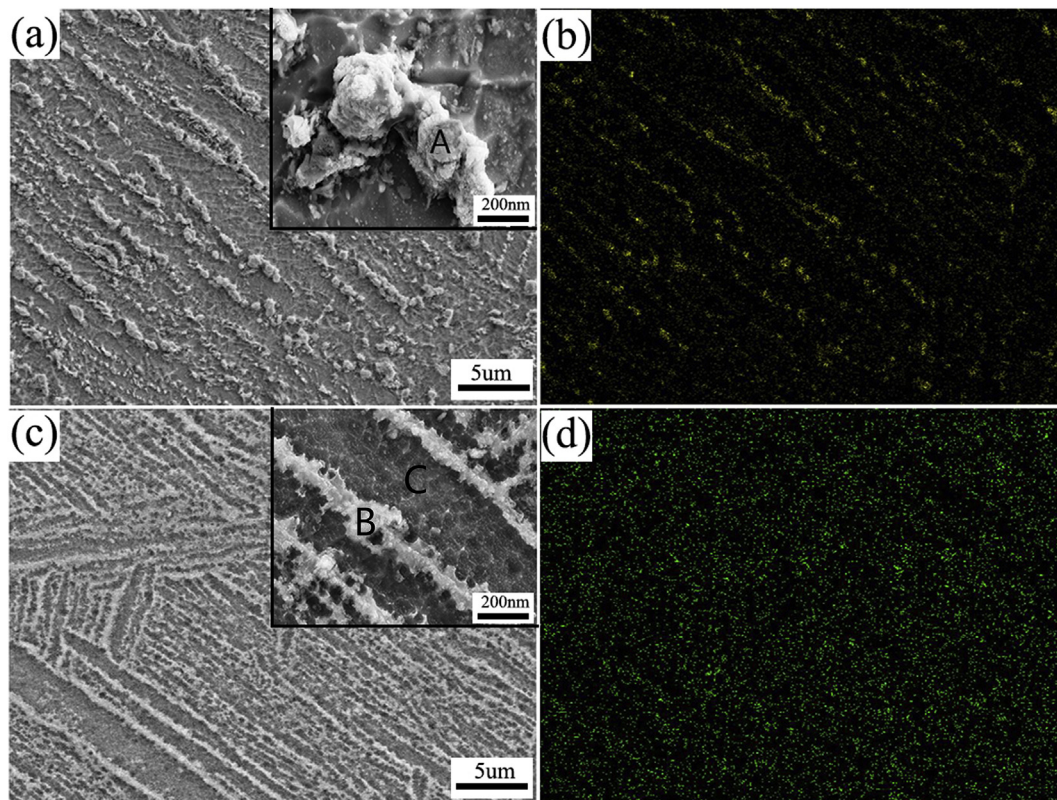


Fig. 3. SEM microstructure of Ti-3Cu alloys under different heat treatments. (a) Ti-3Cu(F), the inserted image shows the high magnification microstructure; (b) Cu element mapping of Ti-3Cu(F); (c) Ti-3Cu(T4), the inserted image shows the high magnification microstructure; (d) Cu element mapping of Ti-3Cu(T4).

significantly but the elongation was obviously decreased from 30.48% to 6.9%. The yield strength and tensile strength was further increased after T6 treatment, and the strength increased slightly with the extension of treatment. However, when the T6 treatment extended from 24 h to 36 h, the elongation was reduced from 10.35% to 6.07% while the yield strength was nearly the same, about 850 MPa.

Taking Ti-3Cu(T6-16) alloy as an example, the fatigue property was assessed under the premise of $R = -1$. From the S-N curve (not shown here), it was determined that the fatigue strengths at cycles of 10^6 and 10^7 were 460 MPa and 450 MPa, respectively.

Fig. 6 shows the fracture surface of Ti-3Cu alloys after different heat treatments. Fig. 6a shows the fracture morphology of Ti-3Cu(F) alloy. It can be seen that there were lots of dimples with different sizes on the fracture surface, corresponding to good plasticity of the forged Ti-3Cu alloy. In Fig. 6b, the crack propagated along the grain boundary which indicated it was a typical brittle fracture after T4 treatment. Fig. 6c shows the fracture morphology of Ti-3Cu(T6-16)

alloy. Some river-like stripes and step-like faults were on the fracture surface, which was a typical cleavage fracture morphology but also a transgranular fracture. Fig. 6d shows the fracture morphology of Ti-3Cu(T6-24) alloy. There were some obvious dimples with small and shallow size at one side of the fracture, while some river-like stripes distributed at other side. It can be inferred that this was a typical quasi-cleavage fracture, but also a kind of brittle fracture. Fig. 6e shows the fracture morphology of Ti-3Cu(T6-36) alloy. There were some small flat fracture surfaces distributed around the fracture which should be caused by the brittle behavior of Ti_2Cu intermetallic.

3.3. Biocorrosion

Fig. 7a and b show OCP and Tafel of Ti-3Cu alloys after different heat treatments. Table 2 summaries the electrochemical data obtained from OCP and Tafel curves. As shown in Fig. 7a, OCP of Ti-Cu alloys all increased with the elapsed time and reached at a stable

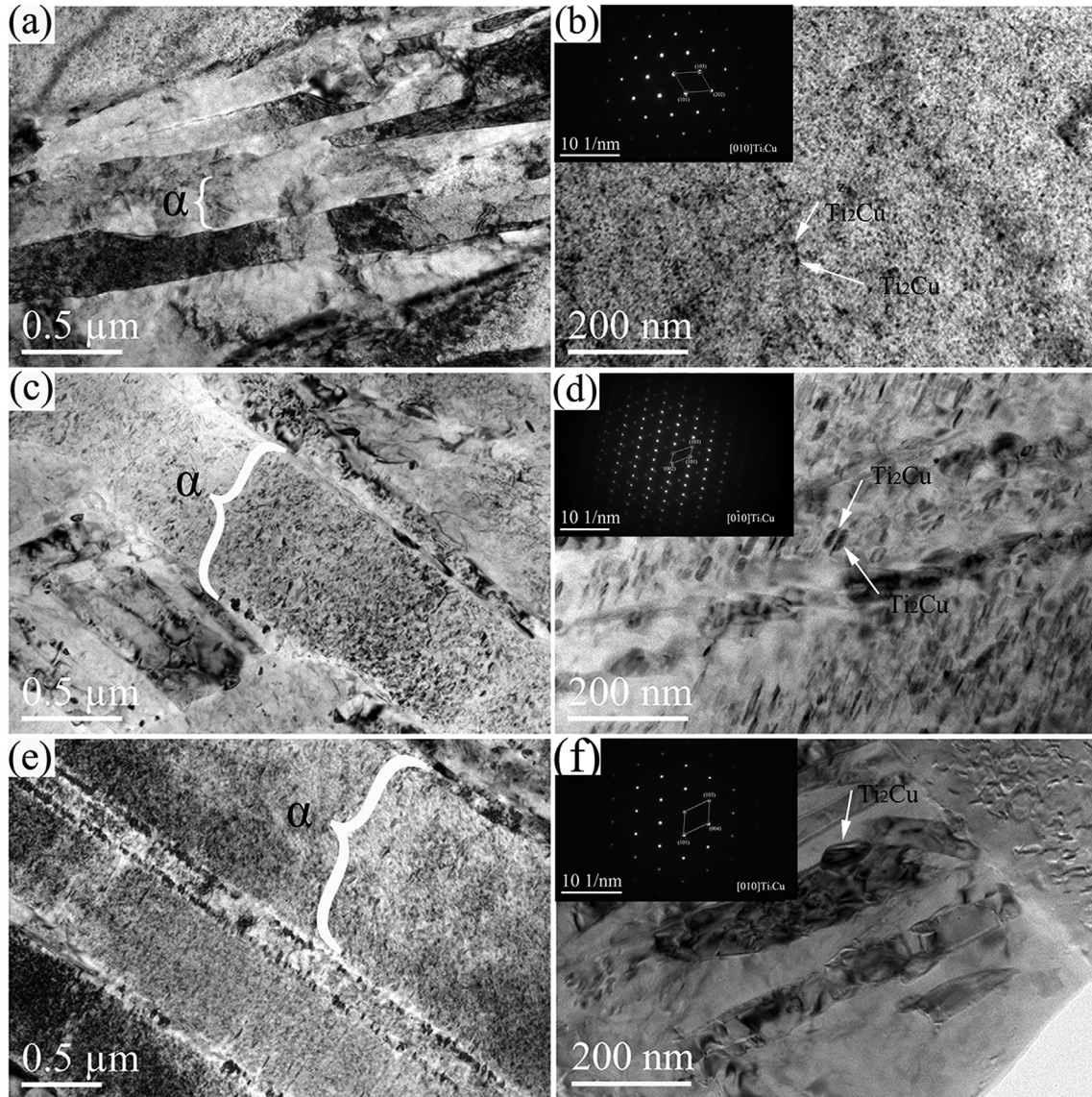


Fig. 4. TEM microstructure of Ti-3Cu alloys under different aging heat treatments. (a) T6-16, (b) high magnification of T6-16, the inserted image shows selected diffraction pattern; (c) T6-24, (d) high magnification of T6-24, the inserted image shows selected diffraction pattern; (e) T6-36, (f) high magnification of T6-36, the inserted image shows selected diffraction pattern.

level, demonstrating that a passive film was formed quickly on the surface. Tafel curves in Fig. 7b also confirms that a protective film was formed quickly on the surface. From the electrochemical data in Table 2, heat treatment, including T4 and T6 treatments, moved E_{ocp} and E_{corr} toward a more noble direction, and reduced the corrosion current density (i_{corr}). No big difference in E_{ocp} , E_{corr} and i_{corr} was found among different heat treatments although slightly lower value in i_{corr} and noble value in E_{ocp} and E_{corr} were observed in T6 treated samples.

Fig. 7c shows Nyquist plot diagram of Ti-3Cu alloys after heat treatment. The impedance was characterized by a large semicircle capacitive loop or a quarter capacitive loop. The Nyquist curves shows one time constant during the frequency range of 0.01–100000 Hz. In comparison with the diameter of the circle arc of Ti-3Cu(F) alloy, it can be found that heat treated Ti-3Cu alloys all showed a much large diameter, especially Ti-3Cu(T6-24) alloy. Fig. 7d shows the Bode phase and Bode plot diagrams of Ti-3Cu alloys. A typical characteristic for the electrochemical impedance spectra of the single layer film was observed. So an equivalent circuit $R_{el}(Q R_p)$ model was used to simulate the structure of the passive film, where R_{el} is the solution resistance in 0.9% NaCl solutions at 37 °C, Q is the passivation film capacitance and R_p is the passivation film resistance. Because it is not an ideal capacitor, the constant phase angle element Q is used to simulate the C. The simulation results were listed in Table 3. From the data, it can be found that after T4 heat treatment, the corrosion resistance (R_p) was increased slightly in comparison with the value of Ti-3Cu(F) alloy. T6 improved the resistance furthermore, but the increase

was limited.

3.4. Antibacterial properties

Fig. 8 shows typical *S. aureus* colonies incubated on Ti-3Cu samples for 24 h and the calculated antibacterial rate. Bacterial colonies incubated directly on the blank control sample and the control sample (cp-Ti) were also shown in Fig. 8a and b for comparison. A large amount of *S. aureus* colonies was observed on the blank control sample and cp-Ti control sample, confirming the fact that both samples do not have antibacterial property. Lots of bacteria were also found on Ti-3Cu(F) alloy, but the number was less than that on cp-Ti sample, indicating that the antibacterial property of Ti-3Cu(F) alloy was not strong. After T4 treatment, the number of bacteria colonies was significantly reduced in comparison with the case of Ti-3Cu(F) samples, as shown in Fig. 8d, exhibiting an antibacterial effect to some extent. Only a dozen of bacterial colonies could be found on the T6 treated Ti-3Cu alloys, as shown in Fig. 8 e to g, indicating strong antibacterial effect.

Fig. 8h shows the change of the calculated antibacterial rate. The forged Ti-3Cu alloy showed the lowest antibacterial rate among Ti-3Cu alloys, about 33%. After T4 treatment, the antibacterial rates increased significantly to 65.2%. Although the antibacterial rate of T4 treated alloys is much higher than the value of the Ti-3Cu alloy, it is still less than the recommended value of 90% as antibacterial materials. However, after T6 treatment, the antibacterial rates increased significantly to 91.32%, 98.54% and 99.32%, for T6-16, T6-24 and T6-36 treated alloys, respectively. According to the Standard

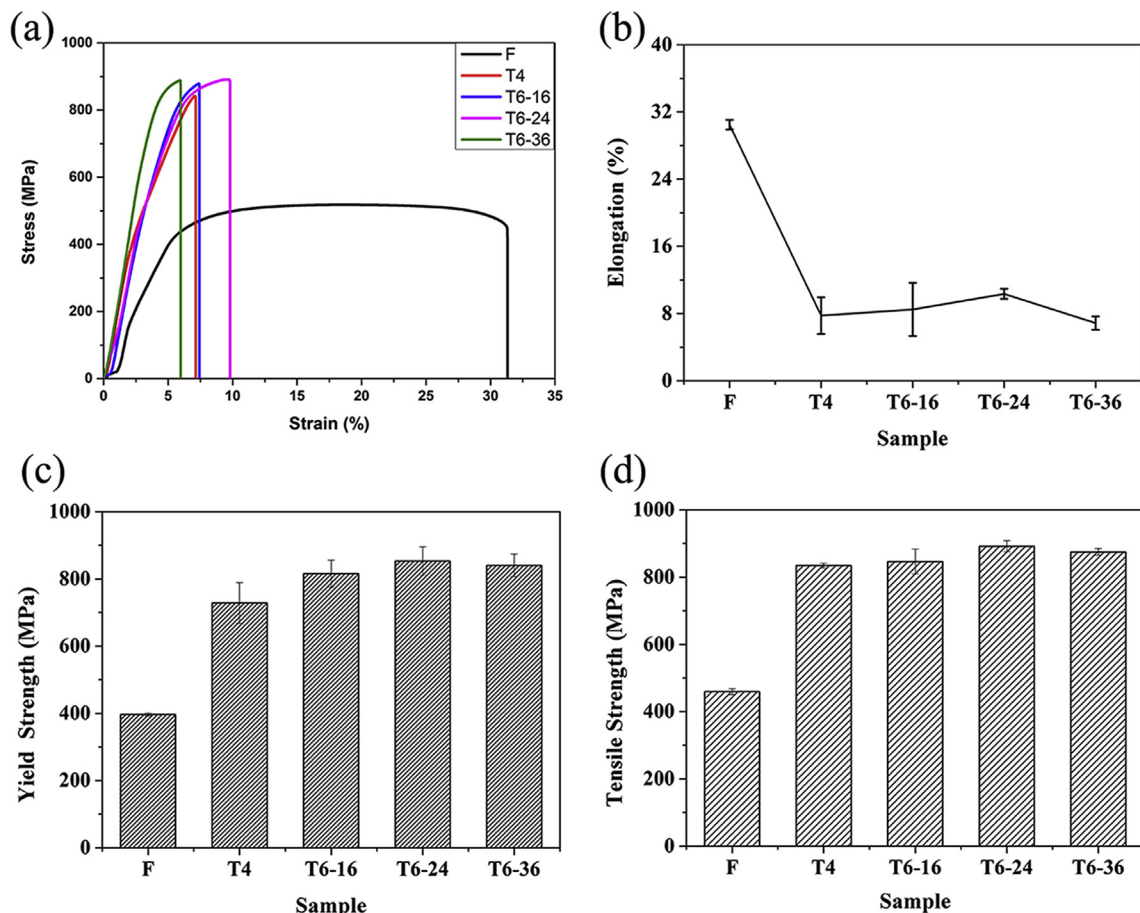


Fig. 5. Tensile properties of Ti-3Cu alloys after different heat treatment. (a) The stress-strain curves, (b) Elongation, (c) Yield strength, (d) Tensile strength.

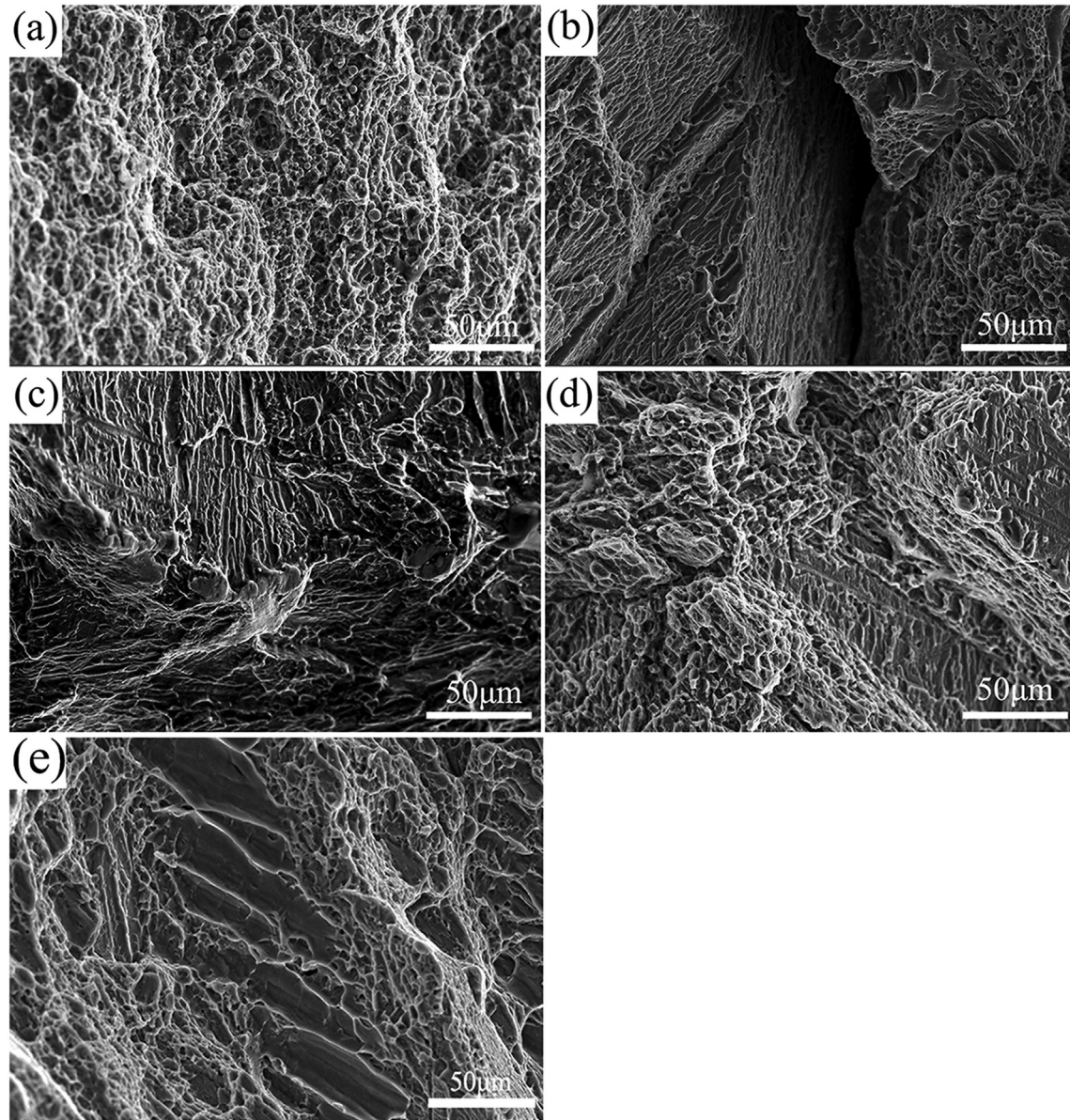


Fig. 6. SEM morphology of the fracture surfaces of Ti-3Cu alloys after different heat treatments. (a) F, (b) T4, (c) T6-16, (d) T6-24, (e) T6-36.

[26], these alloys can be recommended as antibacterial alloys ($R \geq 90\%$) while Ti-3Cu(T6-36) alloy is an alloy with strong antibacterial ability ($R \geq 99\%$).

4. Discussion

As a kind antibacterial implant material, the Ti-Cu alloys should exhibit strong antibacterial ability, but also possess high mechanical properties, good corrosion resistance for long-term loading bearing application. Previous studies have proven that the Cu content of Ti-Cu alloy must be more than 3 wt% for good antibacterial ability [10,14]. The heat treatment can not only improve the mechanical properties but also affect the antibacterial property by changing the state and distribution of Cu. Thus, it is necessary to optimize the microstructure of Ti-3Cu alloy by heat treatment to get high mechanical properties and good antibacterial properties.

Ti-3Cu is a binary alloy system in which copper has a very low solubility in the titanium matrix at room temperature, thus, copper

element will precipitate from matrix as eutectic Ti_2Cu phase as the alloy cools down from melting temperature. Subsequent forging process can significantly refine the grain size as well as secondary phase. XRD results in Fig. 1 clearly shows that Ti_2Cu phase was formed in Ti-3Cu(F) alloy. The high magnification microstructure in Fig. 3 and shows the submicron Ti_2Cu phase precipitated between the lamellar α -phase. T4 treatment dissolved nearly all Cu element in matrix but also brought about large grain size. As a result, the tensile yield strength and the tensile strength were increased significantly in comparison with the values of Ti-3Cu(F) alloy, displaying the strong solid solution strengthening ability of Cu element, but the plasticity was dramatically reduced on the other hand from 30.48% to 6.94%, as shown in Fig. 5. After T6 treatment, nanoscale Ti_2Cu precipitated and distributed uniformly in matrix leads to increases in strength. But with the extension of aging, the increase in strength was limited, for example, as the aging time increased from 16 h to 24 h and to 36 h, the tensile strength increased to 840–900 MPa. No significant difference in strength

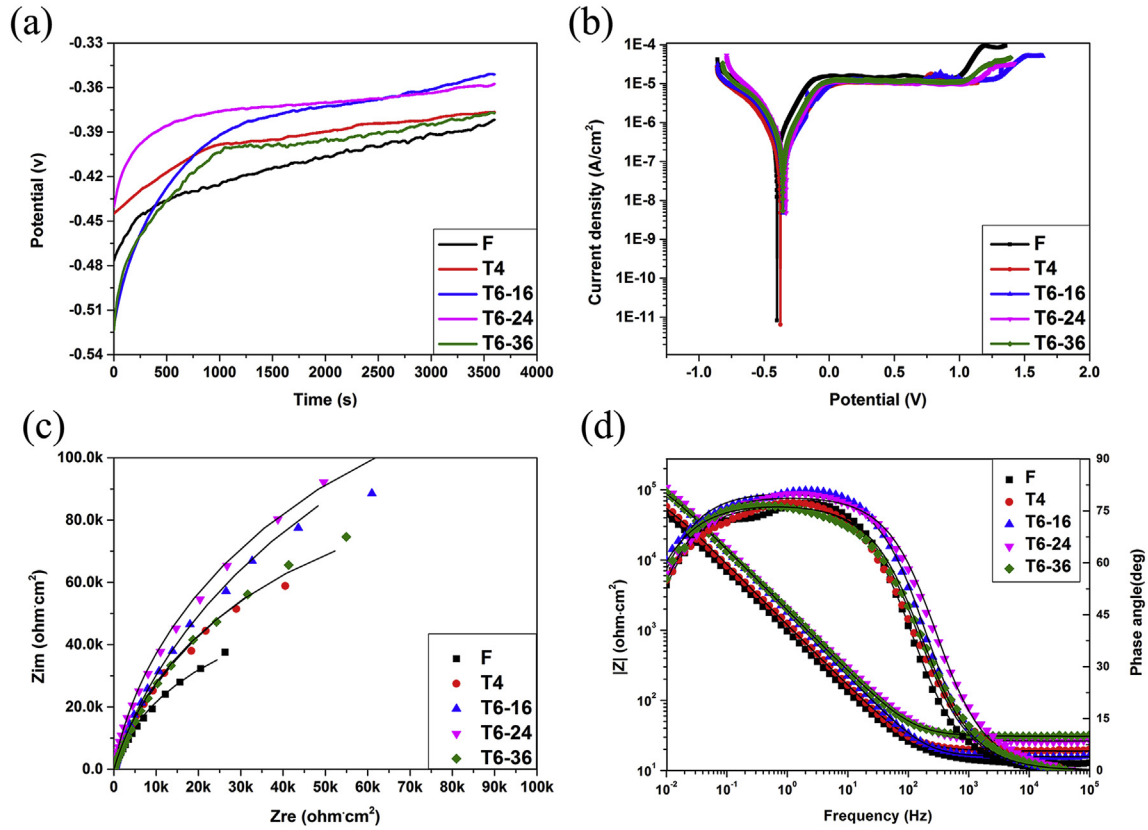


Fig. 7. Electrochemical curves of Ti-3Cu alloys after different heat treatment. (a) Open-circuit potential (OCP), (b) Tafel curves, (c) Nyquist plot diagram, (d) Bode and Bode phase plot diagram.

Table 2
Electrochemical data of Ti-3Cu alloys obtained from OCP and the polarization curves.

Sample condition	E_{ocp} (mv)	E_{corr} (mv)	$i_{corr} \times 10^{-7}$ (A/cm ²)	Corrosion rate (mg/cm ² yr)
F	-386.86 ± 12.93	-400.78 ± 13.27	3.61 ± 0.17	0.052 ± 0.002
T4	-369.70 ± 15.48	-378.42 ± 11.96	1.76 ± 0.23	0.025 ± 0.003
T6-16	-357.59 ± 18.34	-350.74 ± 13.21	1.35 ± 0.12	0.020 ± 0.002
T6-24	-360.12 ± 17.05	-334.93 ± 10.51	0.87 ± 0.08	0.012 ± 0.001
T6-36	-377.26 ± 13.17	-356.12 ± 10.28	1.39 ± 0.16	0.020 ± 0.002

Table 3
Equivalent circuit parameters for EIS spectra.

Sample condition	R_{el} (Ω · cm ²)	CPE (μF cm ⁻²)	n	R_p (× 10 ⁵ Ω cm ²)
F	15.47 ± 3.26	125.54 ± 0.93	0.857 ± 0.005	1.86 ± 0.26
T4	20.25 ± 4.31	113.23 ± 0.87	0.874 ± 0.003	2.04 ± 0.17
T6-16	16.23 ± 3.52	96.15 ± 1.51	0.889 ± 0.002	2.40 ± 0.14
T6-24	21.89 ± 3.29	93.32 ± 1.32	0.897 ± 0.001	2.60 ± 0.21
T6-36	26.51 ± 4.61	104.46 ± 0.89	0.883 ± 0.001	2.13 ± 0.35

was found between T6-36 and T6-24 alloys, but the elongation has a greater decrease of 6.07%, which might be due to the growth up of grain. Takahashi and Ohkubo et al. [27,28] reported that the strength, hardness and abrasion resistance of Ti alloy was improved with the increasing of copper, but the plasticity was reduced, which was attributed to the precipitation of a large number of Ti₂Cu intermetallic compounds after T6 treatment [29,30]. In addition, Ti-3Cu (T6-16) also exhibits very good fatigue strength, as high as 450 MPa at 10⁷ cycles under the premise of R = -1. All these results reveal that heat treatment can change the existing form and distribution of copper in the titanium matrix, in turn enhance the

mechanical properties.

Table 4 summaries the mechanical properties of several commercial biomedical titanium alloys as well as Ti-3Cu alloys. Although the strength of Ti-3Cu is lower than that of Ti-6Al-4V, but far higher than that of pure titanium. In addition, Ti-3Cu(T6) exhibits a high fatigue strength, displaying potential application in bone implant application.

From above results and analyses, it can be deduced that high temperature treatment at 900 °C for 5 h resulted in complete solution of Cu element and increases in strength, but also significant grain growth, which in turn leads to significant reduction in

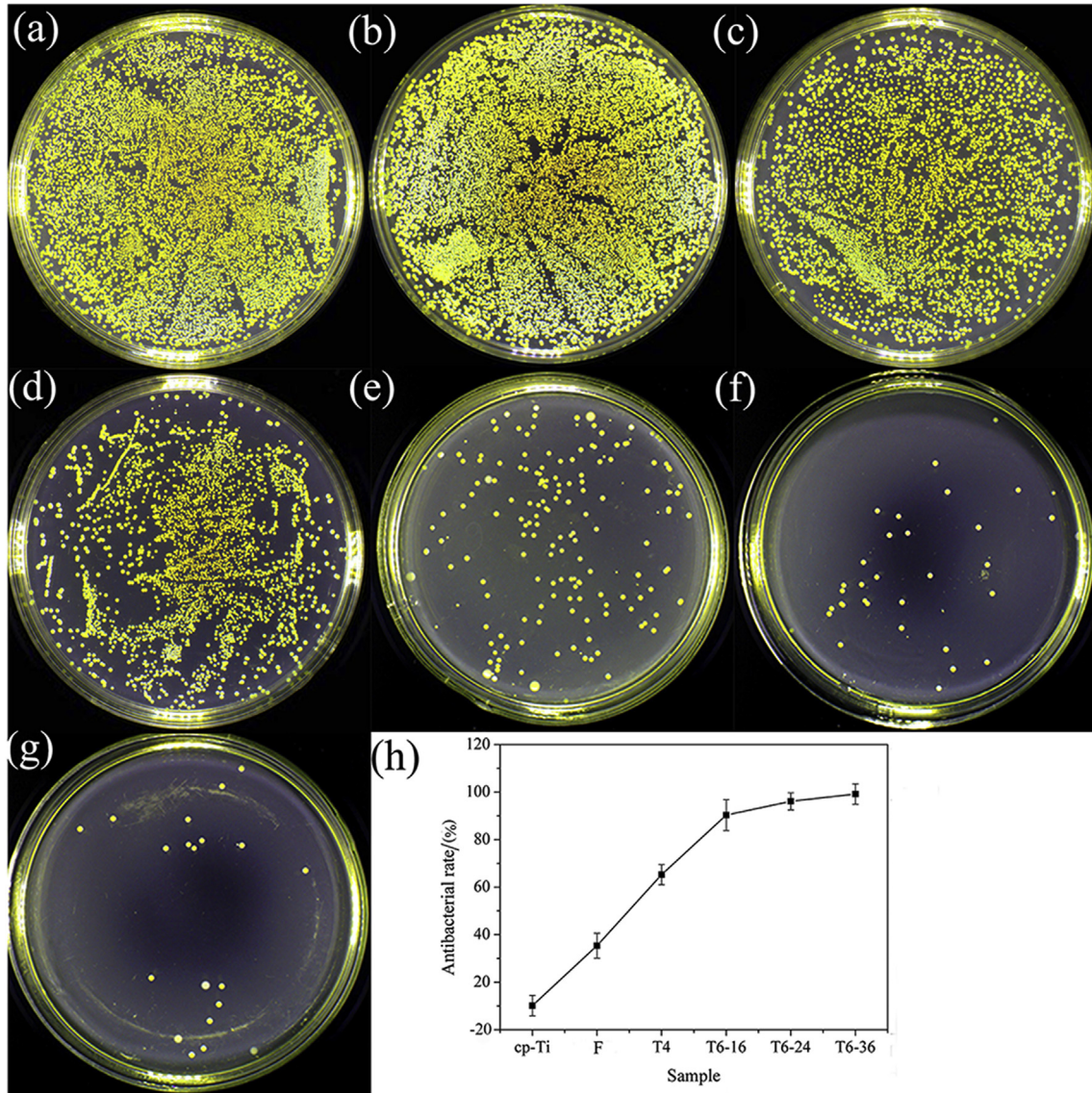


Fig. 8. Typical *S. aureus* colonies after 24 h incubation on different Ti-3Cu alloys and the antibacterial rate of alloys against *S. aureus*. (a) Blank control sample, (b) cp-Ti, (c) Ti-3Cu(F), (d) T4, (e) T6-16, (f) T6-24, (g) T6-36, (h) antibacterial rate of Ti-3Cu alloys.

elongation. So in the next step it is very necessary to optimize the heat treatment to reduce the grain size and the reduction in elongation.

When devices are implanted in human body, the active chloride ions will promote the release of metal ions due to the corrosion reaction, resulting in protein coagulation degeneration, related enzyme inactivation and so on [31]. Good corrosion resistance is

another requirement for implant materials. Commercial pure titanium already shows better anti-corrosion properties in comparison with stainless steel [32,33]. In comparison with cp-Ti, Ti-Cu alloy exhibited slightly better corrosion resistance in five different simulated body fluids, for example, i_{corr} 0.83×10^{-7} A/cm² of Ti-Cu alloy against i_{corr} 1.54×10^{-7} A/cm² of cp-Ti in Hanks solutions [13,19,34]. Electrochemical data in Fig. 7, Tables 2 and 3

Table 4
Mechanical properties of cp-Ti, Ti-6Al-4V and Ti-3Cu alloys.

Alloys (condition)	Y.S. MPa	UTS MPa	Elongation %	Fatigue strength (at 10^7 cycles), MPa	Ref.
cp-Ti (ASTM Grade II)	390–415	520–550	6.5–8.6	274 (20 °C/130 Hz/ annealing)	[22,34–37]
Ti-6Al-4V (Titanium Industries)	880–920	980–1030	1.6–2.8	345 (20 °C/130 Hz/ annealing)	[34–37]
Ti-3Cu(F)	390–400	451–466	29.2–31.8	–	This work
Ti-3Cu(T6-16)	775–840	809–870	5.3–11.5	450 (20 °C/20 Hz)	
Ti-3Cu(T6-24)	809–893	864–895	9.5–11.4	–	
Ti-3Cu(T6-36)	823–890	864–881	6.2–7.5	–	

demonstrate that the corrosion resistance of Ti-3Cu alloy was enhanced by heat treatment, both T4 and T6 treatments. But there is nearly no big difference in the anticorrosion properties between T4 treated alloy and T6 treated alloys as well as among T6 treated alloys. According to the relevant literature [27,35], the formation of the intermetallic compound Ti_2Cu will produce “envelope effect” prevent the alloy from corrosive liquid contact [36], and then strengthen the corrosion resistance of the alloy. Typically, ion release-killing capacity is introduced previously such as antibiotics [37], heavy metals silver ions [38,39], copper ions [40,41], zinc ions [42], which causes microorganisms protein solidification and destructs the bacterial cell synthase activity, and it can influence the bacterial cell division and lead to death. Alternatively contact-killing through increasing effective contact will also strengthen the bactericidal effect, inhibit bacteria adhesion on the surface and avoid the formation of bacterial biofilm [14,43]. For titanium-copper alloys, Ren et al. [12,44] pointed out that titanium alloy with high Cu content could promote the Cu ion release, and hence show strong antibacterial ability. Mei [45] found that Ti-6Al-4V-Cu alloy could disrupt the reactive oxygen species generation and the respiration of bacteria. In this study, Ti-3Cu(F) alloy exhibited an antibacterial ability of about 33% in comparison with cp-Ti. Heat treatment significantly improves the antibacterial ability of Ti-3Cu alloy, e.g. 65% after T4 treatment and >90% after T6 treatment. It was found that with the extension T6 duration, the antibacterial rate increased slightly, such as 91.32% at 16 h to 98.54% at 24 h and then 99.32% at 36 h. For Ti-3Cu(T6) alloy, the Ti_2Cu phase fully precipitated and distributed evenly on the matrix with the extension of aging treatment. As a result, T6 treatment also increases the effective contact between Ti_2Cu phase and bacteria, thus leads to a strong antibacterial effect according to the contact-killing mechanism by inhibiting bacteria adhesion and avoiding the formation of bacterial biofilm. As stated above, the heat treatment slightly enhanced the corrosion resistance of Ti-Cu alloy, therefore, it is believed that the precipitation of Ti_2Cu phase plays a very key role in the great difference in the antibacterial behavior between different alloys.

As a new biomaterial developed for load bearing application, Ti-3Cu alloy exhibited very strong antibacterial ability, high strength and good anticorrosion properties in comparison with cp-Ti and previous study indicated that Ti-Cu alloy exhibited good *in vitro* and *in vivo* cell biocompatibility [15,46], which suggests that Ti-3Cu alloy could have great potential for biomedical application. Results in this study demonstrate that Ti_2Cu phases play an important role in mechanical properties and the antibacterial property of Ti-Cu alloy, so it is possible in the next step to adjust the mechanical and antibacterial properties for different application by adjusting the existing form of Ti_2Cu phase through proper heat treatment.

5. Conclusion

Heat treatment has great influence on the mechanical properties and antibacterial properties of Ti-3Cu alloy by changing the existing formation of Cu element as well as the microstructure of matrix. High temperature treatment contributed to high strength but low plasticity due to the solid solution of Cu element and the coarsening of grain size. Aging treatment provided with high strength and strong antibacterial due to the precipitation of Ti_2Cu . With the increasing of Ti_2Cu phase, the mechanical properties and antibacterial properties increased. Ti-3Cu alloy exhibited very strong antibacterial property and good mechanical properties and corrosion resistance after ageing treatment.

Acknowledgment

The authors would like to acknowledge the financial support from National Natural Science Foundation (no. 81071262, no. 31271024), Funding from North University of China (985 program, N141008001, LZ2014018).

References

- [1] E. Eisenbarth, D. Velten, M. Müller, R. Thull, J. Breme, Biocompatibility of β -stabilizing elements of titanium alloys, *Biomaterials* 25 (2004) 5705–5713.
- [2] M. Niinomi, Recent research and development in titanium alloys for biomedical applications and healthcare goods, *Sci. Technol. Adv. Mater.* 4 (2003) 445.
- [3] T.M. Grupp, T. Weik, W. Bloemer, H.-P. Knaebel, Modular titanium alloy neck adapter failures in hip replacement-failure mode analysis and influence of implant material, *BMC Musculoskel. Disord.* 11 (2010) 3.
- [4] Q. Chen, G.A. Thouas, Metallic implant biomaterials, *Mater. Sci. Eng. R Rep.* 87 (2015) 1–57.
- [5] G. Jin, H. Qin, H. Cao, S. Qian, Y. Zhao, X. Peng, et al., Synergistic effects of dual Zn/Ag ion implantation in osteogenic activity and antibacterial ability of titanium, *Biomaterials* 35 (2014) 7699–7713.
- [6] Y. Wan, G. Xiong, H. Liang, S. Raman, F. He, Y. Huang, Modification of medical metals by ion implantation of copper, *Appl. Surf. Sci.* 253 (2007) 9426–9429.
- [7] J. Cizek, K.A. Khor, Z. Prochazka, Influence of spraying conditions on thermal and velocity properties of plasma sprayed hydroxyapatite, *Mater. Sci. Eng. C* 27 (2007) 340–344.
- [8] J. Shi, C. Chen, H. Yu, S. Zhang, Application of magnetron sputtering for producing bioactive ceramic coatings on implant materials, *Bull. Mater. Sci.* 31 (2008) 877.
- [9] T. Shirai, H. Tsuchiya, T. Shimizu, K. Ohtani, Y. Zen, K. Tomita, Prevention of pin tract infection with titanium-copper alloys, *J. Biomed. Mater. Res. B Appl. Biomater.* 91 (2009) 373–380.
- [10] E. Zhang, F. Li, H. Wang, J. Liu, C. Wang, M. Li, et al., A new antibacterial titanium-copper sintered alloy: preparation and antibacterial property, *Mater. Sci. Eng. C* 33 (2013) 4280–4287.
- [11] J. Liu, F. Li, C. Liu, H. Wang, B. Ren, K. Yang, et al., Effect of Cu content on the antibacterial activity of titanium-copper sintered alloys, *Mater. Sci. Eng. C* 35 (2014) 392–400.
- [12] Z. Ma, L. Ren, R. Liu, K. Yang, Y. Zhang, Z. Liao, et al., Effect of heat treatment on Cu distribution, antibacterial performance and cytotoxicity of Ti-6Al-4V-5Cu alloy, *J. Mater. Sci. Technol.* 31 (2015) 723–732.
- [13] E. Zhang, X. Wang, M. Chen, B. Hou, Effect of the existing form of Cu element on the mechanical properties, bio-corrosion and antibacterial properties of Ti-Cu alloys for biomedical application, *Mater. Sci. Eng. C* 69 (2016) 1210–1221.
- [14] E. Zhang, J. Ren, S. Li, L. Yang, G. Qin, Optimization of mechanical properties, biocorrosion properties and antibacterial properties of as-cast Ti-Cu alloys, *Biomed. Mater.* 11 (2016), 065001.
- [15] E. Zhang, L. Zheng, J. Liu, B. Bai, C. Liu, Influence of Cu content on the cell biocompatibility of Ti-Cu sintered alloys, *Mater. Sci. Eng. C* 46 (2015) 148–157.
- [16] B. Bai, E. Zhang, H. Dong, J. Liu, Biocompatibility of antibacterial Ti-Cu sintered alloy: *in vivo* bone response, *J. Mater. Sci. Mater. Med.* 26 (2015) 265.
- [17] X. Yao, Q. Sun, L. Xiao, J. Sun, Effect of Ti 2 Cu precipitates on mechanical behavior of Ti-2.5 Cu alloy subjected to different heat treatments, *J. Alloy. Comp.* 484 (2009) 196–202.
- [18] S. Souza, C. Afonso, P. Ferrandini, A. Coelho, R. Caram, Effect of cooling rate on Ti-Cu eutectoid alloy microstructure, *Mater. Sci. Eng. C* 29 (2009) 1023–1028.
- [19] E. Zhang, S. Li, J. Ren, L. Zhang, Y. Han, Effect of extrusion processing on the microstructure, mechanical properties, biocorrosion properties and antibacterial properties of Ti-Cu sintered alloys, *Mater. Sci. Eng. C* 69 (2016) 760–768.
- [20] S-l Li, L. Na, X-d Peng, X-y Lu, J-g Li, Fatigue property of hot rolled and cold rolled strips, *J. Iron Steel Res. Int.* 20 (2013) 48–51.
- [21] ASTM E 466-96, Standard Practice for Conducting Force Controlled Constant Amplitude Axial Fatigue Tests of Metallic Materials (West Conshohocken, Pa), 2002.
- [22] Y. Zhao, B. Yang, Probabilistic measurements of the fatigue limit data from a small sampling up-and-down test method, *Int. J. Fatig.* 30 (2008) 2094–2103.
- [23] C. Liu, E. Zhang, Biocorrosion properties of antibacterial Ti-10Cu sintered alloy in several simulated biological solutions, *J. Mater. Sci. Mater. Med.* 26 (2015) 1–12.
- [24] ISO T 10271, Dental Metallic Materials—Corrosion Test Methods, 2001.
- [25] 2591-2003 QTQT, Antimicrobial Plastics: Test for Antimicrobial Activity and Efficacy, 2003.
- [26] 4789.2 G, National Food Safety Standard Food Microbiological Examination: Aerobic Plate Count, 2010.
- [27] M. Takahashi, M. Kikuchi, Y. Takada, O. Okuno, Mechanical properties and microstructures of dental cast Ti-Ag and Ti-Cu alloys, *Dent. Mater. J.* 21 (2002) 270–280.
- [28] C. Ohkubo, I. Shimura, T. Aoki, S. Hanatani, T. Hosoi, M. Hattori, et al., Wear resistance of experimental Ti-Cu alloys, *Biomaterials* 24 (2003) 3377–3381.
- [29] M. Kikuchi, M. Takahashi, T. Okabe, O. Okuno, Grindability of dental cast Ti-Ag

- and Ti-Cu alloys, *Dent. Mater. J.* 22 (2003) 191–205.
- [30] C. Ohkubo, I. Watanabe, J. Ford, H. Nakajima, T. Hosoi, T. Okabe, The machinability of cast titanium and Ti–6Al–4V, *Biomaterials* 21 (2000) 421–428.
- [31] S. Yu, J. Scully, Corrosion and passivity of Ti–13% Nb–13% Zr in comparison to other biomedical implant alloys, *Corrosion* 53 (1997) 965–976.
- [32] M.H. Fathi, M. Salehi, A. Saatchi, V. Mortazavi, S. Moosavi, In vitro corrosion behavior of bioceramic, metallic, and bioceramic–metallic coated stainless steel dental implants, *Dent. Mater.* 19 (2003) 188–198.
- [33] R. Asri, W. Harun, M. Samykano, N. Lah, S. Ghani, F. Tarlochan, et al., Corrosion and surface modification on biocompatible metals: a review, *Mater. Sci. Eng. C* 77 (2017) 1261–1274.
- [34] M. Bao, G. Zheng, X. Wang, E. Zhang, Biocorrosion properties of antibacterial Ti–3Cu alloy in simulated biological environments for biomedical application, *Trans. Nonferrous Metals Soc. China* (2018) (submitted for publication).
- [35] J.-J. Oak, D.V. Louzguine-Luzgin, A. Inoue, Fabrication of Ni-free Ti-based bulk-metallic glassy alloy having potential for application as biomaterial, and investigation of its mechanical properties, corrosion, and crystallization behavior, *J. Mater. Res.* 22 (2007) 1346–1353.
- [36] H. Wei, Y-h Wei, L-f Hou, N. Dang, Correlation of ageing precipitates with the corrosion behaviour of Cu–4wt.% Ti alloys in 3.5 wt.% NaCl solution, *Corrosion Sci.* 111 (2016) 382–390.
- [37] A.R. Shahverdi, A. Fakhimi, H.R. Shahverdi, S. Minaian, Synthesis and effect of silver nanoparticles on the antibacterial activity of different antibiotics against *Staphylococcus aureus* and *Escherichia coli*, *Nanomed. Nanotechnol. Biol. Med.* 3 (2007) 168–171.
- [38] Q. Feng, J. Wu, G. Chen, F. Cui, T. Kim, J. Kim, A mechanistic study of the antibacterial effect of silver ions on *Escherichia coli* and *Staphylococcus aureus*, *J. Biomed. Mater. Res.* 52 (2000) 662–668.
- [39] T. Berger, J. Spadaro, S. Chapin, R. Becker, Electrically generated silver ions: quantitative effects on bacterial and mammalian cells, *Antimicrob. Agents Chemother.* 9 (1976) 357.
- [40] C. Cervantes, F. Gutierrez-Corona, Copper resistance mechanisms in bacteria and fungi, *FEMS (Fed. Eur. Microbiol. Soc.) Microbiol. Rev.* 14 (1994) 121–137.
- [41] C.E. Santo, E.W. Lam, C.G. Elowsky, D. Quaranta, D.W. Domaille, C.J. Chang, et al., Bacterial killing by dry metallic copper surfaces, *Appl. Environ. Microbiol.* 77 (2011) 794–802.
- [42] S. Silver, L.T. Phung, Bacterial heavy metal resistance: new surprises, *Annu. Rev. Microbiol.* 50 (1996) 753–789.
- [43] H. Cakmak, H.S. Taylor, Implantation failure: molecular mechanisms and clinical treatment, *Hum. Reprod. Update* 17 (2011) 242–253.
- [44] L. Ren, Z. Ma, M. Li, Y. Zhang, W. Liu, Z. Liao, et al., Antibacterial properties of Ti–6Al–4V–xCu alloys, *J. Mater. Sci. Technol.* 30 (2014) 699–705.
- [45] M. Li, Z. Ma, Y. Zhu, H. Xia, M. Yao, X. Chu, et al., Toward a molecular understanding of the antibacterial mechanism of copper-bearing titanium alloys against *Staphylococcus aureus*, *Adv. Healthc. Mater.* 5 (2016) 557–566.
- [46] B. Bai, E. Zhang, H. Dong, J. Liu, Biocompatibility of antibacterial Ti–Cu sintered alloy: in vivo bone response, *J. Mater. Sci. Mater. Med.* 26 (2015) 265.